Entropic Segregation of Ring Polymers in Cylindrical Confinement

ARTICLE *in* MACROMOLECULES · JULY 2015

Impact Factor: 5.8 · DOI: 10.1021/acs.macromol.5b00636

2 AUTHORS:

Elena Minina

Universität Stuttgart

8 PUBLICATIONS **12** CITATIONS

SEE PROFILE

Axel Arnold

Universität Stuttgart

56 PUBLICATIONS **1,204** CITATIONS

SEE PROFILE

Macromolecules

Article

pubs.acs.org/Macromolecules

Entropic Segregation of Ring Polymers in Cylindrical Confinement

Elena Minina* and Axel Arnold

Institute for Computational Physics, University of Stuttgart, Stuttgart, Germany

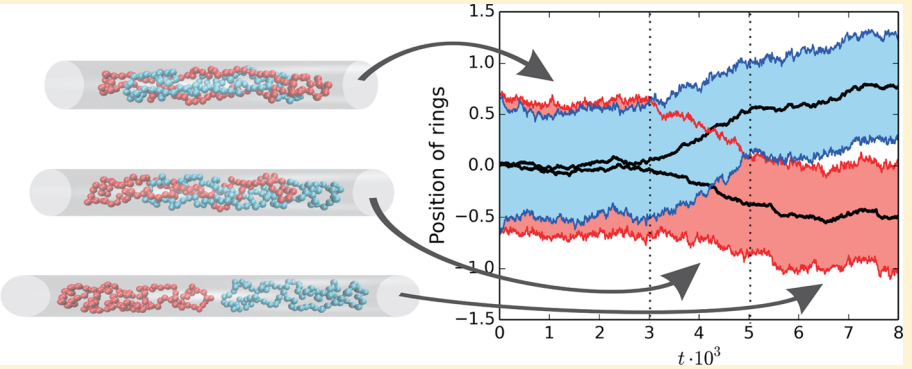

ABSTRACT: Entropic forces tend to demix polymers in confinement, which has been argued to at least facilitate DNA segregation in cylindrical bacteria. Ring polymers as found in modern bacteria such as *Escherichia coli* experience even stronger segregating forces than linear ones due to the fact that rings additionally constrain themselves. Using a territorial "renormalized" Flory approach we obtain a scaling prediction for the segregation force and speed of ring polymers and confirm this prediction by molecular dynamics simulations. The ring topology also affects the induction phase, when the initial symmetry is broken before segregation sets in. We show that the induction time still scales exponentially with the chain length and thus dominates the overall time scale of entropic segregation, although it is significantly shorter than the one for linear chains.

1. INTRODUCTION

Overlap of two polymers in cylindrical confinement significantly reduces conformational entropy, which drives the polymers toward segregation. The interest in this entropic polymer segregation has dramatically increased during the past decade, since it might be one of the driving forces of chromosome segregation in elongated bacteria, e.g., *Escherichia coli*.[1−13] Although real bacteria are full of proteins that also participate in chromosome segregation, this purely entropic effect is an essential part of the process.[11] However, the interplay between the active biological and passive entropic mechanisms of segregation remains to be explored.

Considerable effort has been recently put into understanding entropic segregation. First of all, entropic segregation has been investigated by computer simulations for different confining geometries such as a sphere, two-dimensional box and open and closed cylinders.[1−7,13] There are also studies on the effects of polymer stiffness, crowding, or different polymer topologies.[8−10,12] However, provided that the shape of confinement is sufficiently elongated in one dimension, the polymers inevitably segregate at least partially.[4,6,7,13] The more confined the polymers are, the stronger the segregation forces become. For example, the segregation time of linear chains in cylindrical confinement scales like $N^2D^{0.3}$, where N is the length of the polymer and D is the diameter of the confinement.[2]

Nevertheless, fully overlapping polymers do not necessarily segregate immediately.[2,10] The reason for this is the induction phase, when the initial system symmetry is broken by spontaneous fluctuations. Segregation starts if the polymers' centers of mass get shifted with respect to each other. However, it can happen as well that one polymer gets trapped within the others' coil, so that the polymers cannot segregate. Between this trapped configuration and a configuration that allows entropic segregation a considerable free energy barrier has to be overcome. The height of this barrier and therefore the switching rate scale exponentially with N, so that for long polymers the induction takes much longer than the actual segregation.[14]

It is known that cylindrical confinement induces linear ordering of chain polymers.[1,4,6] Ring polymers due to their topology are even more ordered which enhances segregation.[1,6] In this paper we introduce a generalization of the renormalized Flory approach by Jung et al.,[6] the territorial "renormalized" Flory approach, which allows us to estimate the free energy of many overlapping chains in cylindrical confinement. Using this approach, we investigate the time scales of entropic segregation of rings in open cylindrical confinement, which mimics a growing, idealized simple bacterium of elongated shape. Both segregation and induction take significantly less time for rings compared to linear chains, which we confirm by computer simulations.

Received: March 27, 2015
Revised: June 8, 2015

DOI: 10.1021/acs.macromol.5b00636
Macromolecules XXXX, XXX, XXX−XXX

This article is organized as follows: in section 2, we revisit the theory of entropic segregation using the territorial "renormalized" Flory approach. In section 3, we extend this approach to ring polymers, and in section 4, we compute the induction time of ring polymers. Section 5 then describes the simulation method we use to test our prediction. In section 6, we discuss the obtained results comparing ring and chain polymers, and conclude with section 7.

2. SEGREGATION OF LINEAR CHAINS

We consider two self-avoiding linear polymers confined in an infinitely long cylinder of diameter D as shown in Figure 1,

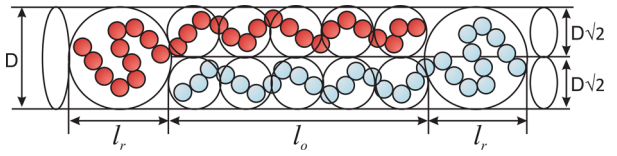

Figure 1. Two linear polymers of equal length in a cylinder of diameter D during segregation. In the overlap region, the cylinder splits into two subcylinders of diameter $D/\sqrt{2}$. The overlapping part spans a distance of l_o along the cylinder; the released parts occupy sections of length l_r each.

where each polymer consists of N monomers of size a. In the following, we compute the free energy of overlap of those two polymers as a function of the center of mass distance R_{c2c}. This implies that we assume that the dynamics are much faster than segregation, so that the latter is a quasi-static process and is therefore unaffected by hydrodynamic interactions. From the obtained free energy we derive the segregating force, which is not constant as previously assumed.[2] These calculations also allow us to explain our territorial "renormalized" Flory approach to compute the overlap energies.

Note that in real bacteria chromosomes are trapped in a shell of finite length rather than an open cylinder, and the cytoplasm is actually crowded by proteins, many of them interacting with DNA. For more complex bacteria, such as *E. coli*, some of these are crucial for replication: due to supercoiling, the two daughter DNA strands in *E. coli* get interlinked during replication, and can only be segregated by the action of specific proteins, namely topoisomerases.[15−18] Nevertheless, our model captures the basic features of entropic segregation, on top of which these proteins act.

First, consider a single polymer in such a cylinder. In the de Gennes blob model,[19] the polymer is modeled as $n_{bl} = N/g$ blobs of size D and g monomers each. Because the blob size is the cylinder diameter, the monomers within a blob do not hit the confinement and behave like in a free polymer, so that $g = (D/a)^{1/\nu}$ with the Flory exponent $\nu \approx 0.6$. The free energy of compression is then

$$\mathcal{F} = \mathcal{F}_{bl} n_{bl} \tag{1}$$

where the free energy per blob $\mathcal{F}_{bl}$ is a nonuniversal constant. For two nonoverlapping polymers, the free energy is just twice this value.

To calculate the free energy of two (partially) overlapping polymers, we use the "renormalized" Flory approach of Jung et al.[6] The idea is that the overlap of two chains in a cylinder of diameter D costs the same amount of free energy as trapping these chains into two subcylinders of reduced diameter $D/\sqrt{2}$ individually. In a way, each polymer occupies its own distinct territory. Now, we split the system into three parts along the main cylindrical axis, with two regions where monomers are already released from the overlap and the overlap region (see Figure 1). In the two outer regions, the free energy can be described by single chains of N_0 monomers each in a cylinder of diameter D. The free energy of the released parts is therefore

$$\mathcal{F}_r(n_0) = 2\mathcal{F}_{bl} n_0 \tag{2}$$

where $n_0 = N_0/g$ is the number of blobs in the overhanging regions.

The overlap region contains the remaining $N - N_0$ monomers of each polymer, which split into $(N - N_0)/g_{sub}$ blobs of size $D/\sqrt{2}$ consisting of $g_{sub}=(D/\sqrt{2}a)^{1/\nu} = g2^{-1/2\nu}$ monomers. Therefore, the free energy of the polymers in the overlap region is

$$\mathcal{F}_o(n_0, n_{bl}) = 2\mathcal{F}_{bl}(n_{bl} - n_0)2^{1/2\nu} \tag{3}$$

leading to a total free energy of

$$\mathcal{F}_{2ch}(n_0, n_{bl}) = 2\mathcal{F}_{bl}[n_0 + (n_{bl} - n_0)2^{1/2\nu}] \tag{4}$$

and a force of

$$F_{2ch} = -\frac{\partial \mathcal{F}_{2ch}(n_0, n_{bl})}{\partial R_{c2c}} = 2\mathcal{F}_{bl}(2^{1/2\nu} - 1)\frac{\partial n_0}{\partial R_{c2c}} \tag{5}$$

where R_{c2c} is the distance between the centers of mass of the two polymers. Note that we need only the partial derivative with respect to n_0, because $n_{bl} = N/g$ does not change during segregation. However, due to the smaller accessible volume, the polymers stretch noticeably in the overlap region, and R_{c2c} does not scale proportional to n_0, as assumed in ref 2.

We are thus left with calculating the right most derivative in eq 5. To this aim we first express R_{c2c} as a function of n_0 and then invert this functional dependence. The length along the cylinder occupied by the released parts is $l_r = n_0 D$, and the length spanned by the overlapping part is

$$l_o = \frac{(N - n_0 g)}{g_{sub}}\frac{D}{\sqrt{2}} = (n_{bl} - n_0)D2^{1/2\nu - 1/2} \tag{6}$$

Taking the system's center of mass as the origin, the centers of mass of the two polymers are

$$R_{c\pm} = \pm\frac{m_r}{2M}(l_o + l_r) \tag{7}$$

where M is the total mass of one polymer, and m_r denotes the mass of polymers in one of the released parts. Because the mass of a polymer is proportional to its number of beads, $m_r/M = n_0/n_{bl}$, and we find

$$R_{c2c} = R_{c+} - R_{c-} = \frac{n_0}{n_{bl}}(l_o + l_r) \tag{8}$$

Substitution of the lengths gives

$$R_{c2c} = \frac{n_0 D}{n_{bl}}[n_0 + (n_{bl} - n_0)2^{1/2\nu - 1/2}] \tag{9}$$

which inverts to

$$n_0(R_{c2c}) = \frac{1}{2[1 - 2^{(1-\nu)/2\nu}]}\left(-n_{bl}2^{(1-\nu)/2\nu} + \sqrt{{n_{bl}}^2 2^{(1-\nu)/\nu} + 4[1 - 2^{(1-\nu)/2\nu}]\frac{R_{c2c} n_{bl}}{D}}\right) \tag{10}$$

DOI: 10.1021/acs.macromol.5b00636
Macromolecules XXXX, XXX, XXX−XXX

Taking the derivative of eq 10 with respect to the R_{c2c} and substituting it into eq 5. we obtain

$$F_{2ch} = \frac{\mathcal{F}_{bl}[2^{1/2\nu} - 1]2^{(3\nu-1)/2\nu}}{D\left(1 + 2[2^{(\nu-1)/2\nu} - 1]\frac{n_0}{n_{bl}}\right)} \tag{11}$$

The ratio n_0/n_{bl} varies from 0 to 1 during segregation, therefore the segregation force is not constant, but increases by 80% toward the end of segregation, see Figure 2. Polymer stretching

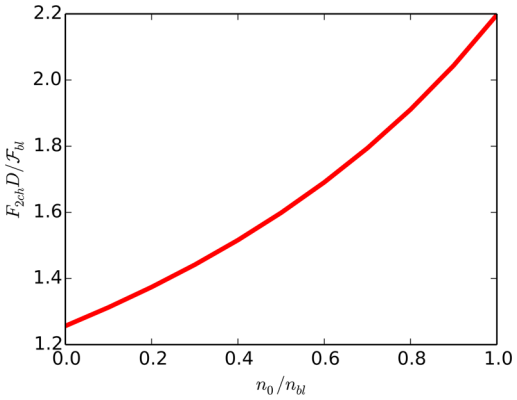

Figure 2. Segregation force of two chains trapped in a cylinder rescaled by the diameter of the cylinder and free energy per one blob $\mathcal{F}_{bl}$ as a function of ratio n_0/n_{bl}.

is clearly observed in the simulation results as presented in Figure 6a–d of ref 2. The overlapping polymers are about 20% longer than they are after segregation, in good agreement with our estimate. Figure 2 in the same reference also shows the acceleration of segregation toward the end of the process. Note that the scaling of the force with respect to diameter of the cylinder is $F \sim 1/D$, irrespective of whether this compression is taken into account. Therefore, the scaling prediction $V \sim 1/(ND)$ for the *average* segregation speed given in ref 2 for a constant segregation force is still a good approximation. Because of that, the segregation time scaling of $t_s \sim N^2D^{2-1/\nu}$ also holds well for long polymers.

3. SEGREGATION OF RINGS

If we replace the two linear chains by rings, they repel stronger due to the additional self-constraining of the rings. To show that, we repeat the calculation of the segregation force for two overlapping rings, using the "renormalized" Flory approach also to take into account the ring topology. In fact, Jung et al. introduced this approach to deal with ring polymers in confinement.

We again split the system into overlapping and non-overlapping regions as for linear chains (see Figure 3). Let us assume that the total number of monomers of one ring released from overlap is N_0. In the "renormalized" Flory approach, such a part of a ring is represented by two parallel subchains of length $N_0/2$ monomers each, which are confined to subcylinders of diameter $D/\sqrt{2}$. A blob of this diameter contains $g_{sub} = g2^{-1/2\nu}$ monomers, and the $N_0/2$ monomers in total occupy a section of length $l_r = N_0g^{-1}D2^{(1-3\nu)/2\nu}$. To calculate the length of overlap, we apply this approach twice, we thus deal with four subchains of length $(N - N_0)/2$, trapped in subcylinders of diameters $D/2$ each. Therefore, the overlap occupies $l_o = (N - N_0)g^{-1}D2^{(1-2\nu)/2\nu}$ along the cylinder.

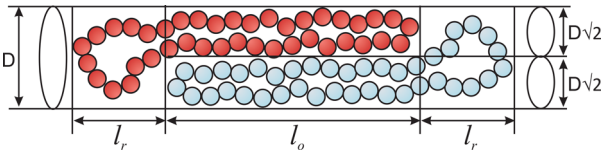

Figure 3. Two segregating ring polymers in an infinitely long cylinder of diameter D. The rings only overlap in the region of width l_o, in the nonoverlapping regions of width l_r the rings are only confined by the cylinder. Jung et al. have shown that a single ring polymer in confinement is equivalent to two single chains in subcylinders of diameter $D/\sqrt{2}$. In the overlap region, the accessible volume for each linear subchain chain is decreased by the presence of three other chains, so that its subcylinder is only $D/2$ wide.

The free energy of two overlapping chains of equal length, whether connected in a ring or disconnected, is almost four times as high as the free energy of a single chain, see eq 3. Since all the contributions to the free energy can be represented as free energies of overlapping chains, the total free energy of two segregating rings scales as the free energy of two chains 4 as follows:

$$\mathcal{F}_{2r}(n_0, n_{bl}) = 2^{1/2\nu}\mathcal{F}_{2ch}(n_0, n_{bl}) \tag{12}$$

where n_0=N_0/g and n_{bl}=N/g. The additional factor 2 in eq 3 drops out, because the length of the linear subchains is half of the ring size. Substituting the ring l_r and l_o into eq 8, we find the distance between the centers of mass distance is

$$\begin{aligned} R^r_{c2c} &= \frac{n_0D}{n_{bl}}2^{1/2\nu-3/2}[n_0 + (n_{bl} - n_0)2^{(1-\nu)/2\nu}] \\ &= 2^{1/2\nu-3/2}R_{c2c} \end{aligned} \tag{13}$$

Then finally the force between two segregating rings is

$$F_{2r} = -\frac{\partial\mathcal{F}_{2r}}{\partial R^r_{c2c}} = -2^{3/2}\frac{\partial\mathcal{F}_{2ch}}{\partial R_{c2c}} = 2^{3/2}F_{2ch} \tag{14}$$

Therefore, rings repel noticeably stronger than linear chains of the same length, by a factor of almost 3. However, the scaling of the free energy or force is unaltered by the ring topology.

Solving the equation of motion for the centers of mass provided by eq 2 in ref 2, we obtain that the segregation speed of rings V^r_{c2c} scales like

$$V^r_{c2c} \sim \frac{2^{3/2}}{DN} \sim 2^{3/2}V^{ch}_{c2c} \tag{15}$$

where V^{ch}_{c2c} denotes the segregation speed of linear chains. Note that this is based on the assumption of a constant force, in practice the segregation accelerates when the polymers have nearly completely segregated. However, just like for linear chains, this describes the scaling of the average segregation speed well, and gives a good estimate for the segregation time. This will be confirmed by our computer simulation data that will be presented in section 6.

4. INDUCTION PHASE

Next, we compute the induction, time, i.e., the time the system takes to break initial symmetry. To this aim, two overhanging regions need to form that consist of approximately a blob, or ≈g monomers. However, there is one additional condition, namely that the two overhanging regions are filled by monomers of different polymers (see Figure 4b). If they belong to the same polymer, these overhanging regions trap the

DOI: 10.1021/acs.macromol.5b00636
Macromolecules XXXX, XXX, XXX–XXX

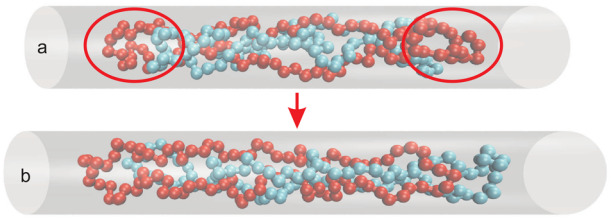

Figure 4. Configurations of ring polymers in a cylinder: (a) One polymer is trapped between the overhanging ends of the other polymer during induction phase. (b) Configuration required for polymer segregation.

other polymer, which inhibits segregation (see Figure 4a). In the latter configuration, the polymer ends have to switch their relative position on one side of the cylinder before segregation can start. Because of a large free energy barrier at full overlap, this reordering is a rare event. The barrier height is proportional to the length of the polymer, therefore the induction time scales exponentially with the number of beads in the polymers,[14] and it is thus much slower than the actual, quadratic segregation time.

Note that we start in our model with two overlapping polymers. In real bacteria, segregation already occurs while the chromosome is replicated at finite speed. Therefore, we performed additional simulations which include polymer replication, see section 6. These simulations show that the induction phase is unaffected by a finite replication rate, if the replication does not take much longer than the segregation. Even in this case, induction is not prevented, but rather shifted by the time replication takes.

Here we compute the induction time of ring polymers following the same approach as ref 14. We consider halves of the two rings that are pinned at the open ends, but can segregate at the other end of the cylinder (see Figure 5). To

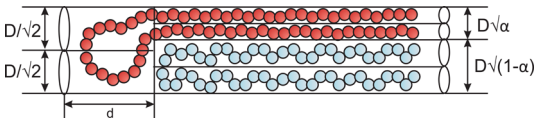

Figure 5. Geometry split of halves of two rings used for investigation of induction time during segregation in a cylinder of diameter D. Typically, one chain hangs over, where d is the length of the overhang region. In the overlap region, the numbers of monomers of the two overlapping chains differ, therefore they occupy different amounts of the available cross-section. This is described by the geometric splitting parameter α.

characterize the switching of the polymer ends, we use the sign of the distance d between the outermost monomers. Like for linear polymers the free energy $\mathcal{F}(N_0)$ of such a system is a sum of three contributions: from the N_0 beads in the overhanging tail of one polymer, from the remaining part of this polymer in the overlap area and from the other polymer, which is completely in the overlap region.

The "renormalized" Flory approach for the ring topology implies that each of these contributions can be written as the free energy of two overlapping linear chains in appropriate subcylinders. However, in this case, the splitting between the subcylinders is no longer equal: the compressed polymer contributes more monomers to the overlap region and therefore also occupies more of the available space. In the following, let α be the fraction of the cross-section occupied by the compressed polymer. Then this half ring is represented by two linear chains of $N/4$ beads each, constrained to a subcylinder of $D\sqrt{\alpha/2}$ (see Figure 5). The chains in the overlap part of the other polymer are confined to diameter $D\sqrt{(1-\alpha)/2}$. Thus, in this general form, the polymers occupy different, but nonoverlapping "territories" across the cylinder, which is why we call this approach "territorial" Flory theory.

Following eq 3, we can simply rescale the free energy for linear chains given by eq 5 from ref 14 and obtain that the total free energy depending on $n_0 = |d|/D$ and $n_{bl} = N/g$ scales like

$$\mathcal{F}(n_0, n_{bl}) = 2^{1/2\nu}\mathcal{F}_{lin}(n_0, n_{bl}) \tag{16}$$

where $\mathcal{F}_{lin}(n_0, n_{bl})$ is the free energy of two linear polymers each composed of $n_{bl}g/2$ monomers, that are confined to a cylinder of diameter D with an overhang of $n_0 g$ monomers. Note that the geometry splitting parameter α remains the same for rings and is given by eq 7 in ref 14.

To determine the free energy difference between full overlap ($d = 0$) and a state with $|d| > 0$, we rewrite the free energy of the configuration with overhanging monomers in terms of $\delta = 2n_0/n_{bl} = 2N_0/N$, i. e. the fraction of overhanging beads compared to the length of the half ring that we consider, and subtract the free energy at full overlap:

$$\frac{\Delta\mathcal{F}(\delta, n_{bl})}{n_{bl}\mathcal{F}_{bl}} = \frac{\mathcal{F}(\delta, n_{bl}) - \mathcal{F}(0, n_{bl})}{n_{bl}\mathcal{F}_{bl}} = 2^{1/2\nu}[\delta + (1-\delta)\alpha^{-1/2\nu} + (1-\alpha)^{-1/2\nu}] \tag{17}$$

The behavior of the this free energy difference is shown in Figure 9 and discussed in detail in section 6, however already here we underline that the free energy difference of rings has the same shape as the free energy difference of linear polymers with a pronounced peak at $\delta = 0$ and a minimum. The position of this minimum corresponds to the equilibrium ratio of overhang and cylinder diameter, and the depth at the minimum is the free energy barrier that the polymers have to overcome when switching positions of the polymer ends. Obviously the free energy barrier for rings also scales like the free energy barrier of chains with an additional prefactor $2^{1/2\nu}$:

$$\mathcal{F}^{r}_{barrier} = 2^{1/2\nu}\mathcal{F}^{ch}_{barrier} = 2^{1/2\nu}\mathcal{F}^{ch}_{\min}\frac{n_{bl}}{2} \tag{18}$$

where $\mathcal{F}^{ch}_{min}$ is the free energy difference per blob of a linear chain between the minimum and full overlap. Note the additional factor 1/2 compared to ref 14, which stems from the fact that here N denotes the full length of the ring, while in ref 14 N denoted half the chain length.

The main scaling of the free energy barrier with the polymer length n_{bl} remains linear. Applying Kramer's or reaction-rate theory,[20] the switching rate of rings is

$$k \sim \mathcal{D}\sqrt{\mathcal{F}''_0\mathcal{F}''_b}\, e^{\beta\mathcal{F}^{r}_{barrier}} \tag{19}$$

where $\beta = 1/k_BT$. $\mathcal{F}''_0$ and $\mathcal{F}''_b$ are the curvatures at the equilibrium distance and at the top of the barrier, respectively. Because of the linear rescaling of the free energy difference for rings with respect to linear chains the curvatures scale like $2^{1/2\nu}/(D^2 n_{bl})$. However, the diffusion constant remains the same as for linear chains $\mathcal{D} \sim 1/g$. Therefore, the switching rate of rings is

DOI: 10.1021/acs.macromol.5b00636
Macromolecules XXXX, XXX, XXX−XXX

$$k \sim \frac{2^{1/2\nu}}{D^2 n_{bl} g} \exp(-\beta \mathcal{F}^{r}_{barrier}) \sim \frac{2^{1/2\nu}}{D^2 N} \exp\left(-\beta 2^{1/2\nu} \mathcal{F}^{ch}_{\min} \frac{N}{2g}\right) \quad (20)$$

The induction time is the mean first passage time of polymers switching roles, which we compute from this as

$$t_{in} \sim \frac{1}{k} \sim D^2 N \exp\left(\beta 2^{1/2\nu} \mathcal{F}^{ch}_{\min} \frac{N}{2g}\right) \quad (21)$$

As in the case of chains, the induction time scales exponentially in the length of the polymers, and dominates the total segregation time for long polymers.

5. SIMULATION METHOD

In order to verify our predictions, we performed molecular dynamics simulations following the approach proposed by Arnold and Jun[2] with some minor corrections required for investigating the induction phase.[14] We consider an open cylinder of diameter D. Inside the cylinder we trap two polymers represented by a bead−spring model. Each polymer consists of N beads of size a with excluded volume interaction modeled by the Weeks−Chandler−Anderson potential:[21]

$$U_{WCA}(r) = k_B T \begin{cases} \left(\frac{a}{r}\right)^{12} - \left(\frac{a}{r}\right)^{6} + \frac{1}{4} & r < \sqrt[6]{2a} \\ 0 & r \geq \sqrt[6]{2a}, \end{cases} \quad (22)$$

where r is the distance between two beads. The same potential is used to describe interactions between the beads and the wall of the cylinder. Each bead is linked by two spring-like bonds to its neighboring beads to create a ring, using the finite extensible nonlinear elastic potential (FENE):

$$U_{FENE}(r) = -\frac{1}{2}\epsilon_F \ln\left[1 - \left(\frac{r}{r_F}\right)^2\right] \quad (23)$$

where $r_F = 1.5a$ is the maximal extension of the bonds and $\epsilon_F = k_F r_F^2 = 22.5 k_B T$ is the interaction strength with spring constant $k_F = 10 k_B T/a^2$. In comparison to ref 2, we slightly reduced the maximal extension in order to prevent excessive bond energies, which occur more frequently in ring systems.

The simulations are computed using the simulation package ESPResSo.[22] We employ a velocity Verlet integrator[23] with fixed time step 0.01 to propagate the system. The temperature of the system is kept constant at $T = 1$ using the Langevin thermostat.

We start the simulations of type Sim. 1 in a perfectly symmetric configuration of two overlapping rings. The rings are cross-linked like a ladder, i. e. the ith beads of both rings are linked. We equilibrate this system, then we remove the cross-linking bonds. Without these additional bonds, the system would start to segregate right away, without equilibrating. Starting from the moment that we cut the cross-links, we compute the centers of mass distance of the rings in order to continue until complete segregation. Simulations of type Sim. 1 are performed for polymers composed of N = 100, 200, 300, 600 beads, and we vary the diameter of the cylinder D = 4, 5, ..., 13. We carry out 100 independent simulations runs for each set of parameters of the system.

In the simulations of type Sim. 2 dedicated to the investigation of the induction phase, we consider only half rings of $N/2$ beads. These half rings are modeled in the same manner as described above using a bead−spring model with initial cross-linked configuration. However, we fix the positions of the beads corresponding to the middle of the full rings to prevent diffusion of the total center of mass. Next to these fixed beads we create a wall on the side opposite to the polymers to mimic the presence of the second half chain. This is important, because otherwise the polymers would back-bend and simply segregate into left and right halves around this fix point. After equilibration of the system we remove the cross-linking bonds and record the signed distance d between the outermost beads of the chains for 1 000 000 time steps. In this set of simulations we also vary the polymer length and diameter of the cylinder D = 4, 5, ..., 13. However, in order to maintain good statistics for all effective blob numbers n_{bl}, we adapt the polymer length to the diameter as $N = n_{bl} g$ for n_{bl} = 1, 2, ..., 20, where $g = (D/a)^{1/\nu}$, $\nu = 0.59$ is the Flory exponent and $a = 1.31$ is the effective persistence length.[24] This results in ring lengths between 6 and 1000 beads.

To check how finite replication rate influences the induction phase, we perform additional simulations (Sim. 3) where we consider two linear chains which again have been cross-linked initially. To model replication, we remove the cross-linking bonds sequentially at a constant rate of f_{rep}. In this manner, we mimic two daughter strands gradually growing from one mother strand, but this approach leads to much more robust molecular dynamics than regularly adding new beads. When the replication is completed, we continue simulations until the end of polymer segregation. As in Sim. 1, we measure the positions of the centers of mass during both replication and segregation. We carried out 200 independent runs for chains of length N = 200, 300 and diameters D = 7, 8. We also tested different replication rates varying f_{rep} from 1 down to 10^{-2}. This spans the entire relevant range, because time 1 corresponds to the relaxation time associated with the motion of individual beads, while at rate 10^{-2} the replication is slower than segregation.

6. RESULTS

Figure 6 shows the measured average segregation speed of two ring as a function of the cylinder diameter D, which is well

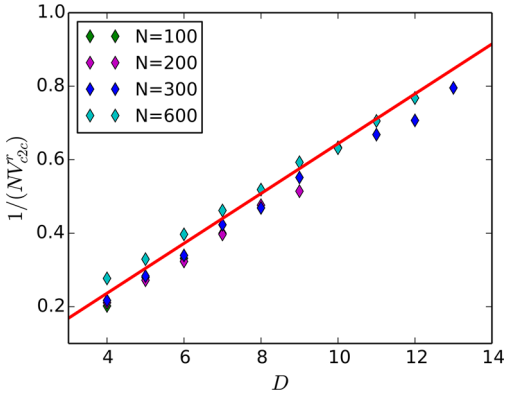

Figure 6. Average speed V^r_{c2c} of two segregating rings of different lengths in a cylinder of diameter D, rescaled by the number of monomers per ring. The colored symbols denote the simulation data of type Sim. 1. The red line is the theoretical prediction from eq 15; the segregation speed of linear polymers V^{lin}_{c2c} was taken from ref 2.

DOI: 10.1021/acs.macromol.5b00636
Macromolecules XXXX, XXX, XXX−XXX

described by eq 15. This confirms that the ring topology speeds up the segregation by a constant factor of $2^{3/2}$ over linear chains of the same length as predicted. Figure 7 shows that the

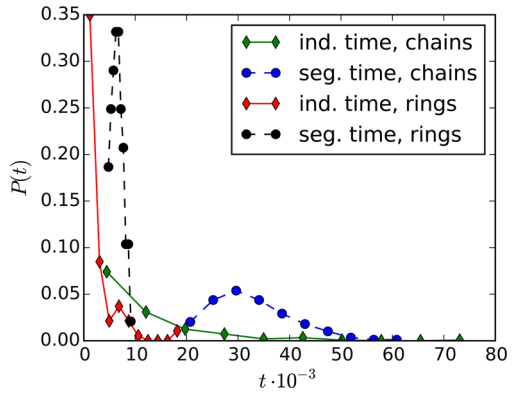

Figure 7. Distribution of induction and segregation time t of two ring polymers obtained from computer simulations Sim. 2 and of two linear polymers obtained from simulations in ref 14. In both systems, each polymer consists of $N = 300$ monomers and the cylinder diameter is $D = 8$.

induction time distribution is also qualitatively unchanged, compared to the one for linear chains. The induction time is exponentially distributed as one would expect from an activated process, so that infrequently the induction can take much longer than the following segregation. However, compared to linear chains, rings spend much less time both for induction and segregation.

The induction phase remains pronounced even for polymers replicating at finite rate, as shown in Figure 8. Fast replication

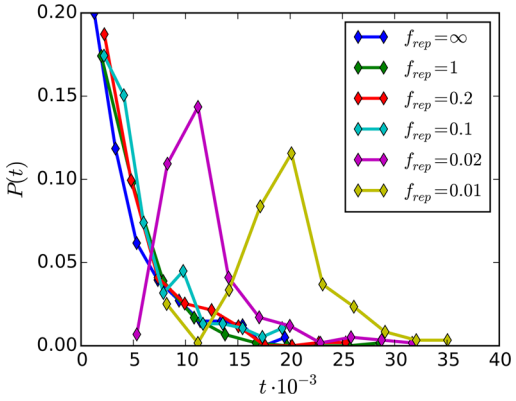

Figure 8. Distribution of induction time t of two linear polymers replicating with replication rate f_{rep} obtained from computer simulations of type Sim. 3. At $f_{rep} = \infty$, the polymers segregate immediately and at $f_{rep} = 1$, the time between two bond releases is the relaxation time of the particle−particle interactions. Each polymer consists of $N = 200$ monomers, the cylinder diameter is $D = 7$. Clearly, the replication rate only has an influence if the replication time exceeds the typical induction time.

($f_{rep} \geq 0.1$ in Figure 8) does not change the induction time distribution compared to immediate replication. At lower rates, the time to full replication determines the segregation time distribution. The most likely segregation time is the one corresponding to the time it takes to full replication, i.e., two independent polymers. Segregation can set in earlier, when about half of the necessary replication time has passed. On the other hand, once the polymers are independent, there is still the exponential distribution observed for immediately replicated polymers. This demonstrates that there is no significant "pre-segregation" of the already replicated parts of the polymers during replication. Even after slow replication, it is still relatively likely to observe situations where one polymers is trapped by the other. Therefore, we believe that the same also holds for ring polymers.

In order to further demonstrate the accurateness of the territorial "renormalized" Flory approach in treating systems of multiple overlapping chains, we compute the free energy

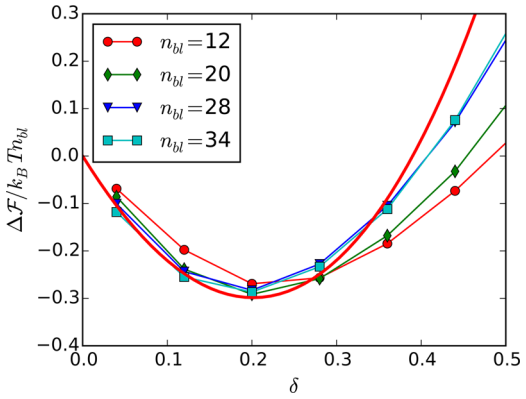

Figure 9. Free energy as a function of $\delta = 2N_0/N$ for ring polymers trapped in a cylinder of diameter $D = 6$. The number of monomers in rings varies from $n_{bl} = 12$ to 34 blobs. The red line denotes the theoretical prediction given by eq 17 with $\mathcal{F}_{bl} = 5k_BT$.

landscape of switching. In Figure 9, we plot an exemplary free energy difference

$$\Delta\mathcal{F}(\delta) = -k_BT[\ln P(\delta) - \ln P(0)] \tag{24}$$

as a function of the ratio $\delta = 2N_0/N$ of overhanging beads to beads in the half chain, which we compute from the probabilities $P(\delta)$ observed during our simulations of type Sim. 2. The free energy landscape between full overlap and the equilibrium position is well predicted by our theory, only for large numbers of overhanging beads deviations occur. This is not unexpected, since this means that for the overhanging chain, only few beads are left for the overlap region, so that the chain becomes fairly stretched and the blob picture breaks down. Again, there are no qualitative differences between rings and chains as reported in ref 14, only the free energy per blob for rings is larger by a factor of $2^{1/\nu}$ due to the additional confinement.

To estimate the free energy barrier that the rings have to overcome to switch their roles, we plot the free energy difference between minimum and the local maximum at $\delta = 0$ as a function of the number of blobs $n_{bl} = N/g$ in Figure 10. As expected, the free energy barrier grows rapidly with the polymer length. We found good agreement between the simulation data and the theoretical prediction eq 18 when inserting the free energy barrier per blob of a linear chain as reported in ref 14 and applying the additional factors for rings.

In the simulations we also measured the switching rate of the polymer ends by counting how many times d changes its sign. These data are shown in Figure 11 as a function of the polymer length in terms of $n_{bl} = N/g$. The red line corresponds to the theoretical prediction eq 20, where the free energy difference

DOI: 10.1021/acs.macromol.5b00636
Macromolecules XXXX, XXX, XXX−XXX

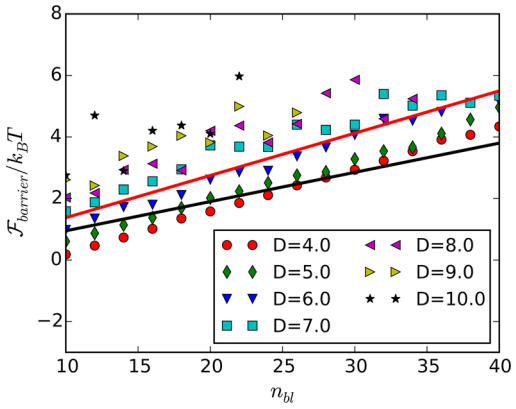

Figure 10. Free energy barrier $\mathcal{F}_{barrier}$ as a function of the number of blobs $n_{bl} = N/g$. Different symbols correspond to different cylinder diameters D. The red line is the theoretical prediction for ring polymers given by eq 18 with the free energy per chain taken from ref 14, the black line is corresponding prediction for linear chains.[14]

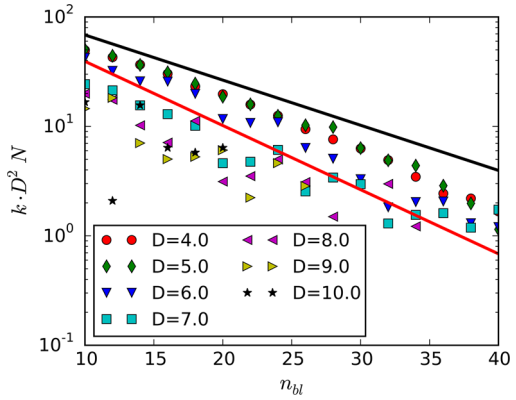

Figure 11. Rate of switching of k rescaled by $1/DN^2$ versus the number of blobs $n_{bl}=N/g$. Different symbols correspond to different cylinder diameters D. The red line is the theoretical prediction from eq 20, with the black line the corresponding prediction for linear chains.[14]

per blob for linear chains $\mathcal{F}^{ch}_{min} = 0.19k_BT$ was taken from ref 14. Again, there is very good agreement between simulation and theory, and the exponential decay of the switching rate with polymer length is clearly visible.

Figure 12 shows the resulting induction time for ring polymers as measured in our simulations of type Sim. 1. By rescaling with a factor of D^2N, all data fall on a single master curve as predicted by eq 21. Here we use the same value of the free energy barrier per blob $\mathcal{F}^{ch}_{min} = 0.19k_BT$ as reported in ref 14 for linear polymers. As for linear chains, the induction time for rings increases exponentially with the chain length. This proves that the different topology of rings and chains has no qualitative influence on the induction time. The only difference is quantitative, in the sense that the exponential growth of the induction time with the polymer length is slower by a factor of $2^{1/2\nu-1} \approx 0.9$ compared than for linear chains of the same length. Thus, the induction time for long rings is much smaller than the one of equally sized linear chains, but still much longer than the actual segregation time.

The deeper reason that the ring topology almost does not play a role lies in the "territorial" behavior of confined polymers. A ring in confinement gets compressed and acts like two parallel polymers that cannot segregate. Otherwise, the two

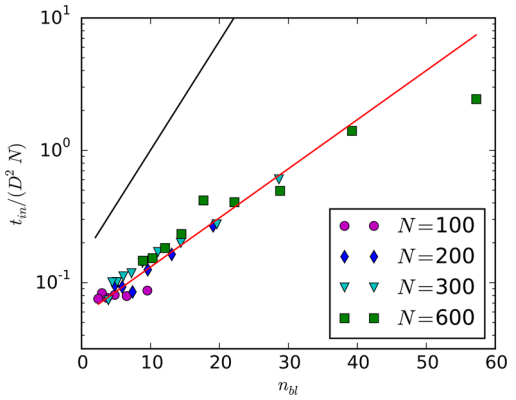

Figure 12. Induction time of ring polymers rescaled by the DN^2 as a function of $n_{bl} = N/g$. Symbols correspond to the simulation data for systems with different total number of monomers N per ring. The red line is the theoretical prediction given by eq 21, the black line is the corresponding prediction for linear chains.[14]

half-rings do not entangle and occupy more or less tube-like territories. Adding a second or more rings or linear chains does not alter this picture: each chain occupies a distinct tube and barely interacts with the other chains apart from reduction of its tube.

7. CONCLUSIONS

We have investigated the entropic segregation of two ring polymers confined in an open cylinder. The main theoretical approach that we have used through out the paper is the territorial "renormalized" Flory approach which turned out to be very powerful for studying overlapping polymers in cylindrical confinement. In this approach, rings are treated as two overlapping linear chains, and the free energy of any number of overlapping chains is simply the sum of the free energies of the underlying chains. This is a consequence of the fact that polymers in cylindrical confinement tend to occupy individual tubes that do not entangle. Therefore, the only interaction is the sharing of accessible volume.

Our computations do not only confirm earlier results[6] that ring topology facilitates segregation, but show that the segregation time scale of rings is strictly proportional to the one of linear chains with the same number of monomers. The induction time grows slower with the polymer length, but still exponentially. Therefore, the induction phase for large rings takes much less time compared to chains, but still much longer than the segregation itself. Thus, it dominates the overall segregation time scale for long polymers.

A finite replication rate does not facilitate segregation. Even at slow rates, trapped configurations are as likely as if the polymers would have been replicated immediately, and segregation does not set in before at least half of the polymers are replicated. This once more confirms that entropic segregation and induction are inevitably linked.

All our theoretical findings are well supported by molecular dynamics computer simulations. This does not only validate our theory, but shows the broad applicability of the territorial "renormalized" Flory theory for studying systems with any number of overlapping polymers of different length in confinement.

DOI: 10.1021/acs.macromol.5b00636
Macromolecules XXXX, XXX, XXX−XXX

AUTHOR INFORMATION

Corresponding Author

*(E.M.) E-mail: minina@icp.uni-stuttgart.de. Telephone: +49 (0)711 68563643. Fax: +49 (0)711 68563658.

Notes

The authors declare no competing financial interest.

ACKNOWLEDGMENTS

The authors thank the German Research Foundation (DFG) for financial support of the project within the collaborative research center SFB 716.

REFERENCES

(1) Jun, S.; Mulder, B. *Proc. Natl. Acad. Sci. U. S. A.* **2006**, *103*, 12388−12393.
(2) Arnold, A.; Jun, S. *Phys. Rev. E* **2007**, *76*, 031901.
(3) Jun, S.; Arnold, A.; Ha, B.-Y. *Phys. Rev. Lett.* **2007**, *98*, 128303.
(4) Jung, Y.; Ha, B.-Y. *Phys. Rev. E* **2010**, *82*, 051926.
(5) Liu, Y.; Chakraborty, B. *Phys. Biol.* **2012**, *9*, 066005.
(6) Jung, Y.; Jeon, C.; Kim, J.; Jeong, H.; Jun, S.; Ha, B.-Y. *Soft Matter* **2012**, *8*, 2095−2102.
(7) Jung, Y.; Kim, J.; Jun, S.; Ha, B.-Y. *Macromolecules* **2012**, *45*, 3256−3262.
(8) Račko, D.; Cifra, P. *J. Chem. Phys.* **2013**, *138*, 184904.
(9) Shin, J.; Cherstvy, A. G.; Metzler, R. *New J. Phys.* **2014**, *16*, 053047.
(10) Polson, J. M.; Montgomery, L. G. *J. Chem. Phys.* **2014**, *141*, 164902.
(11) Pelletier, J.; Halvorsen, K.; Ha, B.-Y.; Paparcone, R.; Sandler, S. J.; Woldringh, C. L.; Wong, W. P.; Jun, S. *Proc. Natl. Acad. Sci. U. S. A.* **2012**, *109*, E2649−E2656.
(12) Kim, J.; Jeon, C.; Jeong, H.; Jung, Y.; Ha, B.-Y. *Soft Matter* **2015**, *11*, 1877−1888.
(13) Ha, B.-Y.; Jung, Y. *Soft Matter* **2015**, *11*, 2333−2352.
(14) Minina, E.; Arnold, A. *Soft Matter* **2014**, *10*, 5836−5841.
(15) Bates, A. D., Maxwell, A., Eds. *DNA Topology*; Oxford University Press: Oxford, U.K., 2005.
(16) Rybenkov, V. V.; Ullsperger, C.; Vologodskii, A. V.; Cozzarelli, N. R. *Science* **1997**, *277*, 690−693.
(17) Wang, J. C. *Annu. Rev. Biochem.* **1996**, *65*, 635−692.
(18) Champoux, J. J. *Annu. Rev. Biochem.* **2001**, *70*, 369−413.
(19) de Gennes, P.-G., Ed. *Scaling Concepts in Polymer Physics*, 1st ed.; Cornell University Press: London, 1979.
(20) Hänggi, P.; Talkner, P.; Borkovec, M. *Rev. Mod. Phys.* **1990**, *62*, 251−341.
(21) Weeks, J. D.; Chandler, D.; Andersen, H. C. *J. Chem. Phys.* **1971**, *54*, 5237−5247.
(22) Limbach, H.; Arnold, A.; Mann, B.; Holm, C. *Comput. Phys. Commun.* **2006**, *174*, 704−727.
(23) Frenkel, D., Smit, B., Eds. *Understanding Molecular Simulation. From Algorithms to Applications*, 2nd ed.; Academic Press: San Diego, CA, 2001.
(24) Arnold, A.; Bozorgui, B.; Frenkel, D.; Ha, B. Y.; Jun, S. *J. Chem. Phys.* **2007**, *127*, 164903.

DOI: 10.1021/acs.macromol.5b00636
Macromolecules XXXX, XXX, XXX−XXX